NON-DIFFUSIVE COMBUSTION WAVES IN INSULATED POROUS MEDIA

[1*]G. Chapiro, [1]D. Marchesin

[1] Instituto Nacional de Matemática Pura e Aplicada (IMPA)

* To whom all correspondence should be addressed.
Address: Est. Dona Castorina, 110, Jardim Botânico, Rio de Janeiro, RJ, Brasil, 22460-320.
Telephone: +55 21 2529-5055
E-mail: grigori@fluid.impa.br

Abstract. Air injection with in-situ combustion has long been considered as a potential technique for displacement and recovery of heavy oil. It utilizes heavy and immobile components of the crude oil as fuel for producing in-place heat necessary for the recovery of upgraded crude oil.

As a laboratory model for air injection, we consider a porous rock cylinder with a homogeneously distributed solid fuel, initially filled with air that is injected at constant rate on the left end of the cylinder. We investigate a forward combustion technique, whereby the combustion starts at the injection end of the cylinder and propagates upstream towards the production end. We neglect air compressibility and heat losses. A bimolecular reaction is assumed to take place between the injected oxygen and the solid fuel, so the region of reaction behaves as a source of heat as well as a sink for the oxygen and fuel. The combustion reaction rate is given by Arrhenius law.

In order to solve the corresponding Riemann problem and find the combustion wave profile some simplifications are commonly used. Many of them are related to the diffusion terms that appear in thermal and gas mass balance laws, for example, one common approximation is to consider high Lewis number. The goal of this work is to discuss the importance of the diffusion terms for the traveling wave solution in these models.

There are different mathematical models describing similar physical phenomena developed in previous works. Here, we compare the solutions of our model with the solutions of earlier models.

Keywords: Co-flow filtration combustion, porous media, traveling wave

1. INTRODUCTION

Air injection with in-situ combustion has long been considered as a potential technique for displacement and recovery of heavy oil reserves (Boberg, 1988; Prats, 1982; Mota et al., 2002). Despite a long history, only a small fraction of the total recovery utilizes this technique. The explanation is (i) until recently, abundance of easily-exploited light-oil reserves, higher-quality resources and cheaper recovery methods; (ii) operational success of the steam injection methods in large reservoirs containing heavy oil. However, most of the production of the Brazilian oil is off-shore and steam injection there is difficult in such sites, from a practical point of view. Other reasons are technical, such as the possibility of front extinction and the necessity of (re-)ignition for sustained propagation within in-situ combustion in the presence of external heat losses (Akkutlu and Yortsos, 2002). Thus mathematical analysis of this problem is important to predict these events.

A large number of studies on the structure of the combustion front have been reported since the 1950s (Akkutlu and Yortsos, 2002; Akkutlu

and Yortsos, 2003; Aldushin et al., 1999; Baily and Larkin, 1960; Benham and Poettmann, 1958; Bousaid and Ramey, 1968; Kumar and Garon, 1991; Schult et al., 1998). However, these studies did not take into account waves that occur in the combustion problem besides the combustion wave. Since there is interaction between the combustion wave and other waves, the solution of the Riemann problem considering all possible waves is relevant. An attempt in this direction can be found in Souza et al., 2006. We also provide further information elsewhere (Chapiro, 2005; Chapiro et al., 2005).

In order to model the in-situ combustion some simplifications are commonly made. For example, Balasuriya et al. (2007) use one-dimensional model and assume limitless access to fuel and constant gas speed, obtaining a system of two conservation laws. Next, the Lewis number is considered high in the analysis of the stability of the combustion front.

In this work we follow the formulation of Souza et al. (2006) explained in the next section. However, we utilize the simplification of neglecting diffusion terms, which is valid when the gas velocity is very high. We also solve the corresponding Riemann problem and obtain the combustion wave profile. It turns out to be almost identical to the one obtained from more complex models with diffusive terms analyzed by using the singular perturbation technique.

2. MATHEMATICAL MODEL

2.1. Formulation

According to Akkutlu and Yortsos, (2002) and Souza et al. (2006), we assume that air is injected at the leftmost part of a mechanically and thermally insulated porous rock cylinder containing solid fuel, so that the flow of mass and energy is one-dimensional. Balance equations are written for the total energy, the total gas mass, the oxygen mass and the fuel mass, and then non-dimensionalized. For the latter, we define the solid fuel density per unit volume, ρ_f, and introduce the extent of conversion depth, $\eta(x,t) = 1 - \rho_f(x,t)/\rho_f^o$ (here ρ_f^o is the initial fuel concentration), such that $\eta = 0$ corresponds to complete availability of fuel and $\eta = 1$ to the complete lack of fuel. The primary dependent variables are the following: the scaled temperature $\theta(x,t)$ (with $\theta = 1$ corresponding to the reservoir temperature), the oxygen mass fraction $Y(x,t)$ within the gaseous phase, the solid fuel density $\eta(x,t)$ and the gas density $\rho_g(\theta, p)$, which is expressed by the ideal gas equation of state in terms of temperature. The gas pressure is considered to vary only slightly; mathematically, we assume that the gas density depends only on temperature. The Darcy velocity $v(x,t)$ is the volumetric flow of gas per unit area. These simplifications yield the non-dimensional ideal gas equation of state $\rho\theta = 1$, where ρ is the non-dimensional gas density.

After introducing dimensionless space and time variables the flow can be modeled by four dimensionless balance equations plus the equation of state (Akkutlu and Yortsos, 2002; Souza et al., 2006):

$$\frac{\partial\theta}{\partial t} + \frac{\partial(a\rho v\theta)}{\partial x} = \frac{\partial^2\theta}{\partial x^2} + q\Phi, \tag{1}$$

$$\phi\frac{\partial(Y\rho)}{\partial t} + \frac{\partial(\rho vY)}{\partial x} = \frac{1}{L_e}\frac{\partial}{\partial x}\left(\rho\frac{\partial Y}{\partial x}\right) - \mu\Phi, \tag{2}$$

$$\phi\frac{\partial\rho}{\partial t} + \frac{\partial(\rho v)}{\partial x} = \mu_g\Phi, \tag{3}$$

$$\frac{\partial\eta}{\partial t} = \Phi, \tag{4}$$

$$\rho\theta = 1, \tag{5}$$

where $\Phi(\theta, Y, \eta)$ is the reaction rate. The nomenclature and typical values of the parameters a, q, ϕ, L_e, α, γ, μ, and μ_g are given in Table 1. The physical domain of the dependent variables θ, Y, a and v is given by:

$$\theta \geq 0, \quad 0 \leq Y \leq 1, \quad 0 \leq \eta \leq 1, \quad v > 0. \tag{6}$$

Table 1. Typical values of dimensionless parameters. (Akkutlu and Yortsos, 2002).

Physical quantity	Symbol	Value
Total heat content of the porous medium	q	1.0121
Stoichiometric coefficients for oxygen	μ	205.8
Stoichiometric coefficients for gaseous products	μ_g	68.19
Lewis number (ratio of thermal and molecular diffusion)	L_e	0.214
Arrhenius number (dimensionless activation energy)	γ	23.69
Dimensionless reaction coefficient	α	0.027
Volumetric heat capacity ratio of the filtrating gas	a	$6.13 \cdot 10^{-4}$
Porosity of the medium	ϕ	0.3

We also want the combustion to be extinguished at reservoir temperature or in the absence of oxygen or fuel, i.e, when at least one of the following conditions is satisfied: $\theta = 1$, $Y = 0$ or $\eta = 1$. These conditions put some restrictions on the form of the reaction rate Φ.

2.2. Simple combustion wave

In this paper we analyze the following simplification of the model (1)-(4), in which the molecular diffusion and thermal heat conductivity are negligible:

$$\frac{\partial \theta}{\partial t} + \frac{\partial (a\rho v\theta)}{\partial x} = q\Phi, \tag{7}$$

$$\phi \frac{\partial (Y\rho)}{\partial t} + \frac{\partial (\rho v Y)}{\partial x} = -\mu\Phi, \tag{8}$$

$$\phi \frac{\partial \rho}{\partial t} + \frac{\partial (\rho v)}{\partial x} = \mu_g \Phi, \tag{9}$$

$$\frac{\partial \eta}{\partial t} = \Phi, \tag{10}$$

$$\rho\theta = 1. \tag{11}$$

We use the first order mass action law combined with the usual Arrhenius law:

$$\Phi = \begin{cases} \alpha Y(1-\eta)e^{-\frac{\gamma}{\theta}} & , \text{for } \theta > 0 \\ 0 & , \text{for } \theta \le 0 \end{cases} \tag{12}$$

Here we focus on the forward combustion front with propagation speed $V > 0$. Physically ahead or behind this wave there is no combustion, i.e, the reaction rate Φ vanishes. Behind the combustion front we consider that there is lack of fuel, by imposing:

$$\theta^b > 0, \quad Y^b = 1, \quad \eta^b = 1, \quad v^b > 0, \tag{13}$$

where the superscript b means burned. Ahead of the combustion front, oxygen levels are depleted, and:

$$\theta^u > 0, \quad Y^u = 0, \quad \eta^u = 0, \quad v^u > 0, \tag{14}$$

where the superscript u means unburned.

We look at the combustion front as a steady traveling wave of system (1)–(4) with propagation speed $V > 0$. The states along such a traveling wave depend only on the moving coordinate $\xi = x - Vt$, i.e, $\theta(x,t) = \hat{\theta}(\xi)$, $Y(x,t) = \hat{Y}(\xi)$ and $\eta(x,t) = \hat{\eta}(\xi)$. Then Eqs. (7)–(11) are transformed into (15)-(18), with hats omitted:

$$\frac{d}{d\xi}\left(av - V\theta\right) = q\Phi, \tag{15}$$

$$\frac{d}{d\xi}\left(\frac{Y(v-\phi V)}{\theta}\right) = -\mu\Phi, \tag{16}$$

$$\frac{d}{d\xi}\left(\frac{v-\phi V}{\theta}\right) = \mu_g\Phi, \tag{17}$$

$$\frac{d}{d\xi}(V\eta) = -\Phi, \tag{18}$$

where Eq. (11) was used to eliminate ρ. The boundary conditions for system (15)–(18) are the conditions (13) at $-\infty$ and (14) at $+\infty$. Notice that (15)-(18) is a first-order ordinary differential equation (ODE) system, which can be rewritten in a matrix form as:

$$\begin{bmatrix} -V & 0 & 0 & a \\ 0 & \tilde{A}_2 & 0 & 0 \\ \tilde{A}_1 & 0 & 0 & 0 \\ 0 & 0 & -V & 0 \end{bmatrix} \begin{bmatrix} \theta_\xi \\ Y_\xi \\ \eta_\xi \\ v_\xi \end{bmatrix} = \begin{bmatrix} q \\ -\mu - Y\mu_g \\ \mu_g - \dfrac{q}{a\theta} \\ 1 \end{bmatrix} \Phi, \tag{19}$$

where $\tilde{A}_1 = (V\phi - v)/\theta^2 + V/a\theta$ and $\tilde{A}_2 = (v - V\phi)/\theta$. The matrix on the left-hand side of Eq. (19) can be inverted, provided that:

$$V \neq 0, \quad V \neq v/\phi, \quad V \neq av/(\theta + a\phi). \tag{20}$$

In Section 6, we will see that these are precisely the speeds of the non-combustion waves presented in (65)-(67). We can solve system (19) and get:

$$\begin{bmatrix} \theta_\xi \\ Y_\xi \\ \eta_\xi \\ v_\xi \end{bmatrix} = \Phi \begin{bmatrix} \dfrac{\theta(a\theta\mu_g - q)}{a(V\phi - v) + V\theta} \\ \dfrac{\mu + \mu_g Y}{V\phi - v}\theta \\ -\dfrac{1}{V} \\ \dfrac{q(V\phi - v) + V\theta^2\mu_g}{a(V\phi - v) + V\theta} \end{bmatrix}. \tag{21}$$

We will prove that the ODE system of Eq. (21) has a solution with boundary conditions defined by (13) and (14) for certain values of V.

3. THE RANKINE-HUGONIOT LOCUS

In order to obtain relations between the boundary conditions (13) and (14) so that system (21) has a solution, we substitute (18) into (15)-(17) obtaining:

$$\frac{d}{d\xi}\left(av - V\theta + qV\eta\right) = 0, \tag{22}$$

$$\frac{d}{d\xi}\left(\frac{(v - \phi V)Y}{\theta} - \mu V\eta\right) = 0, \tag{23}$$

$$\frac{d}{d\xi}\left(\frac{v - \phi V}{\theta} + \mu_g V\eta\right) = 0. \tag{24}$$

This means that the quantities inside the derivatives are constant in ξ, thus their value at some finite ξ is the same as at $\xi \to \infty$.

$$av - V\theta + qV\eta = av^u - V\theta^u - qV\eta^u, \tag{25}$$

$$\frac{vY}{\theta} - \frac{\phi VY}{\theta} - \mu V\eta = \frac{v^u Y^u}{\theta^u} - \frac{\phi VY^u}{\theta^u} - \mu V\eta^u, \tag{26}$$

$$\frac{v}{\theta} - \frac{\phi V}{\theta} + \mu_g V\eta = \frac{v^u}{\theta^u} - \frac{\phi V}{\theta^u} + \mu_g V\eta^u. \tag{27}$$

Next we can take the limit $\xi \to -\infty$ of the left-hand side of Eqs. (25)-(27), and substitute condition (13) on the left-hand side and condition (14) on the right-hand side of such system to obtain:

$$av^u - V\theta^u = av^b - V\theta^b + qV, \tag{28}$$

$$0 = \frac{v^b - \phi V}{\theta^b} - \mu V, \tag{29}$$

$$\frac{v^u - \phi V}{\theta^u} = \frac{v^b - \phi V}{\theta^b} + \mu_g V. \tag{30}$$

Physically, it is reasonable to assume that we know the temperature at the right of the combustion wave (θ^u) as well as the Darcy velocity (v^b) of the injected gas. This choice will be useful in Section 6, so we have three unknowns (θ^b, v^u, V) and three equations (28)-(30). From Eq. (29):

$$\theta^b = \frac{v^b - \phi V}{\mu V}. \tag{31}$$

Subtracting (29) from (30):

$$v^u = \phi V + V\theta^u(\mu + \mu_g). \tag{32}$$

Now we substitute (31) and (32) in (28) and obtain:

$$\mu V\theta^u + \mu a v^b - v^b + \phi V + \mu q V - a\mu\phi V = a\mu(\mu + \mu_g)V\theta^u. \tag{33}$$

We define $J(\theta^u) = \mu\theta^u + \mu q - \phi a\mu + \phi - a\mu^2\theta^u - a\mu\mu_g\theta^u$; one can verify that $J(\theta^u) > 0$ for the values of the constants given in Table 1 for any $\theta^u > 0$. Using this J and (33) we obtain:

$$V = \frac{(1 - a\mu)v^b}{J(\theta^u)}. \tag{34}$$

Now we have θ^b and v^u defined in (31) and (32) as functions of θ^u and $V = V(\theta^u, v^b)$ defined by (34).

4. COMBUSTION PROFILE

In this section we use the boundary conditions defined in Section 3 and the equations (22)-(24) to obtain θ, Y, v as functions of η and of the parameters, and substitute the result in the equation for η_ξ in (21). Then we compare these results to the solutions for the system (1)-(5) obtained by singular perturbation techniques in Chapiro (2005) and Chapiro et al. (2005).

4.1. Ordinary differential equations for the profile

From equations (25)-(27) we obtain:

$$av - V\theta = av^u - V\theta^u - qV\eta, \tag{35}$$

$$\frac{(v-\phi V)}{\theta} Y = \mu V \eta, \tag{36}$$

$$v = \phi V - \mu_g V\eta\theta + \frac{\theta}{\theta^u}(v^u - \phi V) = \phi V - \mu_g V\eta\theta + V\theta(\mu + \mu_g), \tag{37}$$

where we have used (32). Substituting v from (37) and v^u from (32) into (35), dividing by V and simplifying, we obtain:

$$\theta = \frac{a\theta^u(\mu+\mu_g) - \theta^u - q\eta}{a(\mu+\mu_g-\mu_g\eta)-1}. \tag{38}$$

Using (37) in (36) we get:

$$Y = \frac{\mu\eta}{\mu+\mu_g-\mu_g\eta}. \tag{39}$$

Finally, using (38), (39) and (12) we can rewrite the equation for η_ξ in (21) as:

$$\eta_\xi = \frac{\alpha Y(1-\eta)}{-V} exp\left(\frac{-\gamma}{\theta}\right) = \frac{-\alpha\mu\eta(1-\eta)}{(\mu+\mu_g-\mu_g\eta)V} exp\left(\gamma\frac{1-a(\mu+\mu_g-\mu_g\eta)}{a\theta^u(\mu+\mu_g)-\theta^u-q\eta}\right). \tag{40}$$

We can solve this ODE with any initial condition $\eta(0)=\eta^0$, where $0<\eta^0<1$ and substitute the result into the equations (38), (39) and (37) for θ, Y, v and obtain the combustion wave profile. Solving these equations with MATLAB with initial condition $\eta^0 = 0.5$, we obtain the wave profile shown on the left side of Figure 1.

In Chapiro et al. (2005), the approximation of order zero for combustion wave profile for the system (1)-(4) was obtained using singular perturbation techniques. One can see the result on the right side of Figure 1. It agrees with the solution of system (7)-(10), i.e., the solution of the ODE (40). The plots are in the same scale.

4.2. Approximation explicit solution

We have solved the ODE (40) numerically, however sometimes it is useful to have explicit approximations of the solution. To obtain such approximation we use the fact that $a<<1$ to approximate the exponent of (40):

$$\gamma\frac{1-a(\mu+\mu_g-\mu_g\eta)}{a(\mu+\mu_g)-1-q\eta} \approx \frac{-\gamma}{1+q\eta}. \tag{41}$$

Now we rewrite the pre-exponential factor as:

$$-\frac{\alpha}{V}\frac{\mu\eta(1-\eta)}{\mu+\mu_g-\mu_g\eta} = \frac{A\eta(1-\eta)}{B-\eta}, \tag{42}$$

where $A=(-\alpha\mu)/(V\mu_g)$, $B=1+\mu/\mu_g$. The ODE for the approximate solution is:

$$\frac{d\eta}{d\xi} = \frac{A\eta(1-\eta)}{B-\eta}\exp\left(\frac{-\gamma}{1+q\eta}\right). \tag{43}$$

We use the exponential integral function (Press et al., 1989) and obtain the implicit solution of ODE (43):

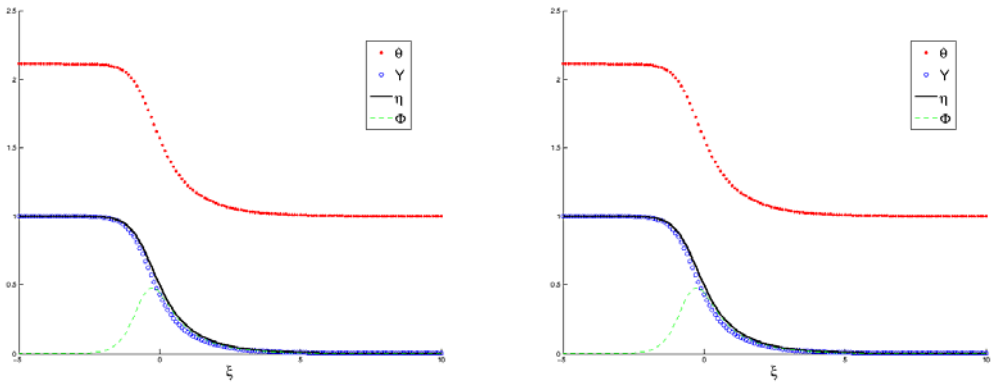

Figure 1. On the left the traveling wave solution of the system (40). On the right the first order approximation of the traveling wave of the system (1)-(4) from Chapiro et al. (2005). Variables: θ (dotted line), Y (circles), η (solid) and the combustion rate Φ (dashed) as functions of ξ. We use $\gamma = 2$.

$$-\frac{1}{A}\left(E_1\left(\frac{-\gamma}{1+q\bar{\eta}}\right)-E_1\left(\frac{-\gamma}{1+q\eta}\right)\right)+$$
$$\frac{Be^{\gamma}}{A}\left(E_1\left(\frac{\gamma q\bar{\eta}}{1+q\bar{\eta}}\right)-E_1\left(\frac{\gamma q\eta}{1+q\eta}\right)\right)-$$
$$\frac{(B-1)}{A}\exp(\frac{\gamma}{1+q})\left(E_1\left(\frac{\gamma q(\bar{\eta}-1)}{(1+q)(1+q\bar{\eta})}\right)-\right. \quad (44)$$
$$\left.E_1\left(\frac{\gamma q(\eta-1)}{(1+q)(1+q\eta)}\right)\right)=\xi.$$

Now we notice that not all terms in (44) are important. First we combine all constants:

$$\tilde{K}=\frac{1}{A}\left[-E_1\left(\frac{-\gamma}{1+q\bar{\eta}}\right)+Be^{\gamma}E_1\left(\frac{\gamma q\bar{\eta}}{1+q\bar{\eta}}\right)-\right. \quad (45)$$
$$\left.-(B-1)\exp(\frac{\gamma}{1+q})E_1\left(\frac{\gamma q(\bar{\eta}-1)}{(1+q)(1+q\bar{\eta})}\right)\right]$$

and drop the term $E_1(-\gamma/(1+q\eta))$, as it is small compared to the other ones, obtaining:

$$-Be^{\gamma}E_1\left(\frac{\gamma q\eta}{1+q\eta}\right)+(B-1)\exp(\frac{\gamma}{1+q}) \quad (46)$$
$$E_1\left(\frac{\gamma q(\eta-1)}{(1+q)(1+q\eta)}\right)=(\xi-\tilde{K})A.$$

We can compare the solution of (46) with the numerical solution of (40) on Figure 2. The solution in (46) is implicit and it is not very easy to work with. We simplify it utilizing the series expansion of the exponential integral function (Press et al., 1989), and taking the real part to get:

$$(\xi-\tilde{K})A=Be^{\gamma}\log\left(\frac{\gamma q\eta}{1+q\eta}\right)- \quad (47)$$
$$(B-1)\exp(\frac{\gamma}{1+q})\log\left(\frac{\gamma q(\eta-1)}{(1+q)(1+q\eta)}\right).$$

We compare the solution of (47) with the numerical solution of (40) in Figure 2.

4.3. The dimensional solution

Until now, we studied the non-dimensional equations and performed non-dimensional analysis, however for applications it is important to know the characteristic values of our solution in actual units.

Looking at the fuel consumption rate equation (40) we conclude that the reaction occurs close to the region where $\eta\approx 0.5$; from the numerical experiments we can conclude that it happens for $0.4<\eta<0.8$. From (47) with some simplifications we get:

$$\delta\xi=\frac{2V}{\alpha}\exp(\frac{\gamma}{1+q})+\frac{V\mu_g}{2\alpha\mu}e^{\gamma}+\frac{V}{2\alpha}e^{\gamma}\approx \quad (48)$$
$$\frac{2V}{\alpha}\exp(\frac{\gamma}{1+q}).$$

The last approximation is not accurate, however here we are interested just in the approximated length. Substituting the values from Table 1 we get $\delta\xi\approx 3.5\cdot 10^4$.

In order to obtain physical values we introduce characteristic values for length l^* (that will be analyzed later) and speed v^* (we can put it as $1m/s.$), thus characteristic time will be $t^*=l^*/v^*$. We define $l^*=\alpha_s/v^*$, where α_s is the effective thermal conductivity

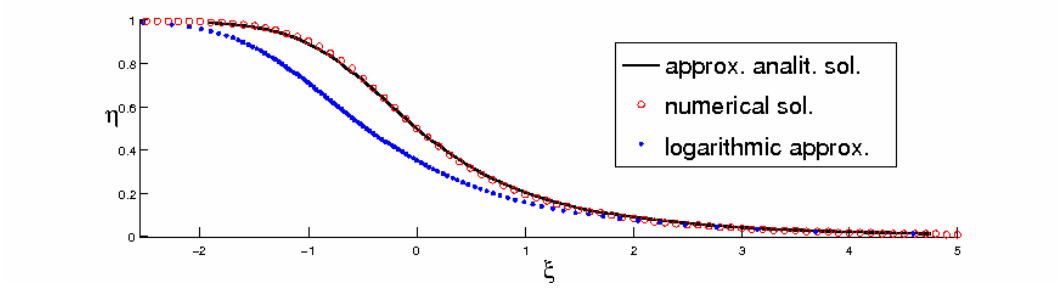

Figure 2. Numerical solution of (40) (solid), analytical solution of an approximate ODE (43) (circles) and logarithmic approximation (47) (dotted) used to calculate the characteristic length. All plots use $\gamma=2.0$.

$\alpha_s = \tilde{\lambda}/((1-\phi)c_s\rho_s) = 4.301\cdot10^{-7}\,m^2/s$. Now the characteristic length will be $l^* = \alpha_s / v^* \approx 4.301\cdot10^{-7}/v^*$, where v^* is some reference value for injection speed (but not the actual injection speed).

We recover all dimensional variables: temperature $\tilde{T} = \tilde{T}_0\theta$, where $\tilde{T}_0$ is the reservoir temperature; time $\tilde{t} = \hat{t}t^* = \hat{t}\alpha_s/(v^*)^2 = 4.301\cdot10^{-7}\hat{t}/(v^*)^2$; length $\tilde{x} = l^*\hat{x} = 4.301\cdot10^{-7}\hat{x}/v^*$[m]; oxygen $\tilde{Y} = Y^iY$, where $Y^i = 0.23$ is the injected oxygen fraction in total gas mass; and fuel $\rho_f = (1-\eta)\rho_f^0$, where $\rho_f^0 = 19.2182$ $[kg/m^3]$ is the initial fuel density.

Finally, the characteristic length is $\tilde{x} = 4.301\cdot10^{-7}\hat{x} \approx 1.5\cdot10^{-2}[m]$. This result is compatible with experimental data (Essenhigh, 1981).

5. TESTING THE SOLUTION WITHIN THE COMBUSTION WAVE

In order to solve the linear system (19), the restrictions (20) need to be satisfied for V. On the other hand our physical model imposes other restrictions related to the boundary conditions (13) and (14) for the combustion waves. Verifying that these restrictions are satisfied is the goal of this section.

5.1. Monotonicity

Here we will prove that the solutions $\theta(\xi)$, $Y(\xi)$ and $\eta(\xi)$ given by the equations of θ_ξ, Y_ξ, and η_ξ in (21) are monotonic. The combustion rate defined by (12) is always positive, thus from (21) or (40) we see that $\eta(\xi)$ is monotone decreasing.

In order to prove that $\theta(\xi)$ is monotonic we use (38) obtaining:

$$\frac{d\theta}{d\eta} = \frac{KV(a\mu_g\theta^u - q)}{(K - a\mu_g V\eta\theta^u)^2}, \qquad (49)$$

where $K = av^u - V\theta^u - a\phi V$. The numerator of (49) is independent of η and the denominator is positive. As $\eta(\xi)$ is monotonic, $\theta(\xi)$ is monotone decreasing and thus θ^b from (31) satisfies $\theta^b > \theta^u$.

In order to prove the monotonicity of $Y(\xi)$ we use (39) to obtain $dY/d\eta$:

$$\frac{dY}{d\eta} = \frac{\mu V\theta^u(v-\phi V)}{((v-\phi V) - \mu_g V\eta\theta^u)^2}. \qquad (50)$$

As the numerator of (50) is constant in η and the denominator is always positive, the function $Y(\xi)$ is monotonic. As $Y^u < Y^b$ we conclude that $Y(\xi)$ is monotone decreasing.

Now we will prove that for all ξ, $v^u < v(\xi) < v^b$ where v^b and v^u are given by (32). First of all we assume that $\theta^u < \mu q/\mu_g \approx 4$, so $\mu_g\theta^u < \mu q$ and as $0 \le \eta \le 1$, $\mu_g(\theta^u + \eta q) < q(\mu+\mu_g)$. We multiply the last equation by η and add $\theta^u(\mu+\mu_g)[1-a(\mu+\mu_g-\eta\mu_g)]$ to both sides of the inequality; some algebra leads to $\theta^u(\mu+\mu_g) - a\theta^u(\mu+\mu_g)(\mu+\mu_g-\mu_g\eta) \le (\mu+\mu_g)\theta^u + (\mu+\mu_g)q\eta - (\mu+\mu_g)^2 a\theta^u - \mu_g\eta(\theta^u+\eta q) + a\mu_g\eta\theta^u(\mu+\mu_g)$. If we group terms we get $[1-a(\mu+\mu_g-\mu_g\eta)]\theta^u(\mu+\mu_g) \le (\mu+\mu_g-\mu_g\eta)[\theta^u + q\eta - a\theta^u(\mu+\mu_g)]$. Using (38), the following inequality holds:

$$\theta^u(\mu+\mu_g) \le (\mu+\mu_g-\mu_g\eta)\frac{\theta^u + q\eta - a\theta^u(\mu+\mu_g)}{1-a(\mu+\mu_g-\mu_g\eta)} = (\mu+\mu_g-\mu_g\eta)\theta. \qquad (51)$$

Multiplying by V and using (32) and (37), we obtain that $v^u \le v(\xi)$.

In order to verify that $v(\xi) < v^b$ one uses the values of Table 1 to verify:

$$\theta^u > a\left((\mu_g/\mu)\theta^u(\mu+\mu_g) + 2(\mu+\mu_g)\theta^u + (\mu+\mu_g)q\right). \qquad (52)$$

We multiply by μ and add $\mu(q + a\mu_g q\eta) + \mu_g\eta\theta^u$ to both sides of (52), obtaining:

$$\mu_g\eta(a\theta^u(\mu+\mu_g)+q\eta+a\mu q\eta)+$$
$$\mu(2a(\mu+\mu_g)\theta^u+a(\mu+\mu_g)q)< \quad (53)$$
$$\mu(\theta^u+q+a\mu_g q\eta)+\mu_g\eta\theta^u.$$

Organizing (53) in a different manner:

$$(1-a\mu)(a\theta^u(\mu+\mu_g)\mu_g\eta-\theta^u\mu_g\eta-q\eta^2\mu_g)<$$
$$(\mu\theta^u+\mu q-a\mu^2\theta^u-a\mu\mu_g\theta^u)(1-a\phi+a\mu_g\eta)=$$
$$(J-(\mu+\mu_g)(1-a\mu))(1-a\phi+a\mu_g\eta). \quad (54)$$

Dividing by $(1-a\mu)$ and using (34):

$$\mu_g\eta(a\theta^u(\mu+\mu_g)-\theta^u-q\eta))<$$
$$(\frac{v^b}{V}-(\mu+\mu_g))(1-a\phi+a\mu_g\eta). \quad (55)$$

Using (38) and (35) we obtain:

$$v=\phi V-\mu_g V\eta\theta^u+V\theta(\mu+\mu_g)\le v^b. \quad (56)$$

At this point we have proved that the functions $\theta(\xi)$, $Y(\xi)$, $\eta(\xi)$ are monotonic and $v^u<v(\xi)<v^b$, so they satisfy the boundary conditions given in (13) and (14). In other words the wave speed V is physically admissible.

5.2. Verifying the characteristic inequalities

In this subsection we prove that V in (34) satisfies the restrictions (20). Obviously, V satisfies (20a). For (20b,c) we will show:

$$\frac{av(\xi)}{a\phi+\theta(\xi)}<V<\frac{v(\xi)}{\phi}. \quad (57)$$

In Section 5.1 we proved that the function θ is monotone decreasing in ξ and v satisfies $v^u\le v(\xi)\le v^b$, so we have for all values of ξ:

$$\frac{av(\xi)}{a\phi+\theta(\xi)}\le\frac{av^u}{a\phi+\theta^u}<\frac{v^b}{\phi}\le\frac{v(\xi)}{\phi}. \quad (58)$$

Therefore instead of (57a) we verify whether V satisfies

$$\frac{av^u)}{a\phi+\theta^u}\le V\le\frac{v^b}{\phi}. \quad (59)$$

For the values given in Table 1 we have $0<1-a(\mu+\mu_g)$, multiplying by μ we have $0<\mu\theta^u-a\mu^2\theta^u-a\mu\mu_g\theta^u$ and also $\phi+\mu q-\mu a\phi<\mu\theta^u+\mu q-\phi a\mu+\phi-a\mu^2\theta^u-a\mu\mu_g\theta^u=J(\theta^u)$. From the last equation using (34) and $(1-a\mu)>0$ we obtain $V(\phi+\mu q-\mu a\phi)<v^b(1-a\mu)$. It follows that $V(\mu\theta^u+\phi+\mu q)-v^b(1-a\mu)<V(\mu a\phi+\mu\theta^u)$, dividing by $a\mu$ and using (32) we obtain $av^u<V(a\phi+\theta^u)$. Dividing the last equation by $(a\phi+\theta^u)$ we obtain (59a).

In order to prove (59b) we notice that $\theta^u+q-a\mu\theta^u-a\mu_g\theta^u>0$ and then $(1-a\mu)\phi<J$, where $J=\mu\theta^u+\mu q-\phi a\mu+\phi-a\mu^2\theta^u-a\mu\mu_g\theta^u$; multiplying the last inequality by v^b and dividing it by $J>0$ we get:

$$\frac{(1-a\mu)v^b}{J}<\frac{v^b}{\phi}; \quad (60)$$

Here we conclude that the solution of the system (19) for V defined in (34) always exists and that V always satisfies (59) and consequently (57).

6. NON-COMBUSTION WAVES AND WAVE SEQUENCES

In the absence of combustion, the source terms representing mass transfer or sensible heat generation containing the factor Φ vanish on the right hand side of system (7)–(11). Of course Φ vanishes for $Y\equiv 0$ or $\eta\equiv 1$. We consider smooth solutions and expand the derivatives in the remaining terms in (7)-(10), manipulate (8), (9) and finally use (11) to eliminate ρ, obtaining:

$$\frac{\partial\theta}{\partial t}+a\frac{\partial v}{\partial x}=0, \quad (61)$$
$$\phi\frac{\partial Y}{\partial t}+v\frac{\partial Y}{\partial x}=0, \quad (62)$$
$$\left(\frac{\theta}{a}+\phi\right)\frac{\partial\theta}{\partial t}+v\frac{\partial\theta}{\partial x}=0, \quad (63)$$
$$\frac{\partial\eta}{\partial t}=0. \quad (64)$$

In increasing order, the characteristic speeds of system (61)-(64) and the corresponding characteristic vectors are (Souza et al., 2006):

$$\lambda^\eta=0, \qquad (0,0,1,0)^T, \quad (65)$$

$$\lambda^{\theta} = a\frac{\nu}{\theta + a\phi}, \qquad (1,0,0,\frac{\nu}{\theta + a\phi})^T, \tag{66}$$

$$\lambda^{Y} = \nu/\phi, \qquad (0,1,0,0)^T. \tag{67}$$

It is easy to see that all characteristic speeds are constant along the integral curves defined by the corresponding characteristic vector fields, which means that all the waves are contact discontinuities; of course, they satisfy the Rankine-Hugoniot conditions for (7)-(11). The characteristic speed λ^{η} corresponds to an immobile discontinuity along which only η varies, λ^{θ} corresponds to a thermal discontinuity along which θ and ν vary and λ^{Y} corresponds to a gas composition discontinuity along which only Y varies.

In section 5.2 we have seen that the wave speeds in (65)-(67) are all different and satisfy (57). Now we will describe the wave sequence in the Riemann solution under conditions (13) and (14) surrounding the combustion front (Souza et al., 2006).

We indicate by U the vector containing the variables $U = (\theta, Y, \eta, \nu)$. In our case (hot upstream combustion) the thermal wave precedes the combustion wave ($\lambda^{\theta}(U^b) < V$), there is no temperature change ahead the combustion wave, which means that $\theta^b > \theta^u$. Because of the inequalities $\lambda^{\eta} < \lambda^{\theta} < \lambda^{Y}$, the wave sequence in the Riemann solution consists of an immobile fuel shock, a thermal shock with speed λ^{θ} and a combustion front with speed V. The gas composition wave with speed λ^{Y} does not effectively exist due to the complete oxygen consumption assumed in the boundary condition (14). We denote this sequence of waves by means of the following convention:

$$U^i \xrightarrow{\lambda^{\eta}} U^1 \xrightarrow{\lambda^{\theta}} U^b \xrightarrow{V} U^u. \tag{68}$$

The state $U^i = (\theta^i, 1, 0, \nu^i)$ denotes the injection conditions, $U^1 = (\theta^i, 1, 1, \nu^i)$ denotes an intermediate state in the burned region, while $U^b = (\theta^b, 1, 1, \nu^b)$ and $U^u = (\theta^u, 0, 0, \nu^u)$ are the burned and the unburned states surrounding the combustion front.

We summarize our results in the following theorem, which provides formulae for all the states as well as speeds for combustion and non-combustion waves in the wave sequence (68) for the Riemann solution. In this theorem we have fixed reservoir temperature at $\theta^u = 1$.

Theorem 1: *Assume that in the wave sequence for the Riemann solution of (7)-(12) there is a hot upstream combustion wave with left and right states satisfying (13)-(14) and* $\theta^b > \theta^u$. *For given injection conditions* $U^i = (\theta^i, 1, 0, \nu^i)$, *with* $\theta^i > 0$, $\nu^i > 0$ *and reservoir temperature* θ^u, *the constant states and the speeds of all waves in the wave sequence (68) are uniquely determined.*

Proof: First of all, as shown by Souza et al. (2006), the characteristic pair (66) corresponds to a contact discontinuity and there is a relationship between the injection conditions

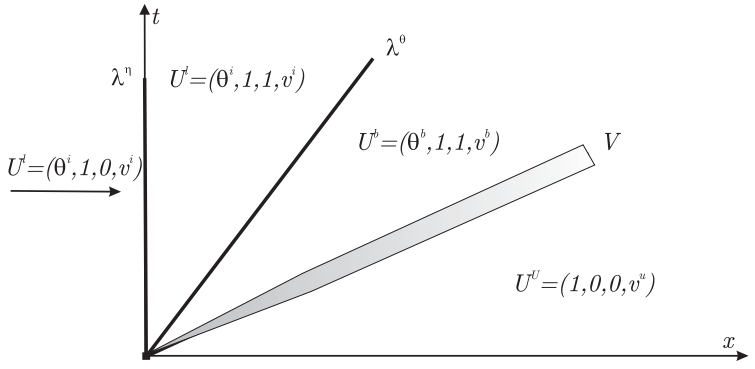

Figure 3. Regions separated by immobile, thermal wave and combustion waves in the Riemann solution. Values of θ, Y, η and ν in each region.

U^i and the burned state U^b:

$$a\frac{v^i}{\theta^i + a\phi} = a\frac{v^b}{\theta^b + a\phi}. \tag{69}$$

Now we get four independent relationships (31), (32) (34), and (69) between the parameters θ^b, θ^u, θ^i, v^b, v^u and v^i, so the result of the theorem is to be expected. In Figure 3 we see that the speeds and the intermediate states in the wave sequence (68) are determined as follows.

Substituting θ^b from (31) in (69) it follows that

$$\left(a\phi + \frac{v^b - \phi V}{\mu V}\right)v^i = av^b(\theta^i + a\phi);$$
$$v^b = \frac{\phi V(a\mu - 1)v^i}{\mu V(\theta^i + a\phi) - v^i}. \tag{70}$$

Using v^b from (70) we can use (34) to obtain V; next we use (31) and (32) to obtain θ^b and v^u as functions of θ^i, θ^u and v^i. This completes the proof of Theorem 1.

7. CONCLUSIONS

In this paper we describe an interesting and simple non-diffusive gas-solid co-flow combustion model. We obtain the wave profile and solve the corresponding Riemann problem. Comparing these results to ones obtained in previous works for the more general model we conclude that the diffusion terms do not affect qualitatively the propagation of the combustion wave.

ACKNOWLEDGEMENTS

We would like to thank Alexei Maylibaev and Jesuíno Aparecido de Souza for important contributions and discussions. We thank the referees for corrections.

This work was performed at IMPA as part of the Ph.D. thesis of Grigori Chapiro with support of CAPES and ANP/PRH-32.

This work was supported in part by CNPq under Grants 304168/2006-8, 472067/2006-0, 491148/2005-4, FAPERJ E-26/152.525/2006 and FINEP 01.06.1043.00.

REFERENCES

Akkutlu, I.Y.; Yortsos, Y.C. The Effect of Heterogeneity on In-situ Combustion: The Propagation of Combustion Fronts in Layered Porous Media. J. Pet. Tech., 54, 6:56-56, 2002.

Akkutlu, I.Y.; Yortsos, Y.C. The Dynamics of In-situ Combustion Fronts in Porous Media. J. Combustion and Flame, 134 (3), 229-247, 2003.

Aldushin, A.P.; Rumanov, I.E.; Matkowsky, B.J. Maximal Energy Accumulation in a Superadiabatic Filtration Combustion Wave. J. Combustion and Flame, 118, 76-90, 1999.

Baily, H.R.; Larkin, B.K. Conduction-convection in Underground Combustion, Petroleum Trans. AIME, 217, 321-331, 1960.

Balasuriya, S.; Gottwald, G.A.; Hornibrook, J.; Lafortune, S. High Lewis Number Combustion Wavefronts: a perturbative melnikov analysis. SIAM Journal on Applied Mathematics, 67(2), 464-486, 2007.

Benham, A.L.; Poettmann, F.H. The Thermal Recovery Process – An Analysis of Laboratory Combustion Data. Petroleum Trans. AIME, 213, 406-408, 1958.

Boberg, T.C. Thermal Methods of Oil Recovery. An Exxon Monograph Series, 1988.

Bousaid, I.S.; Ramey, Jr., H.J. Oxidation of Crude Oil in Porous Media. Soc. Pet. Eng. J., 8, 2:137-148, 1968.

Chapiro, G. Singular Perturbation Applied to Combustion Waves in Porous Media. MSc Thesis, IMPA, 2005 (in Portuguese). (Preprint version in http://www.preprint.impa.br/Shadows/SERIE_B/2005/9.html).

Chapiro, G.; Mailybaev, A.A.; Marchesin, D.; Souza, A.J. Singular Perturbation in Combustion Waves for Gaseous Flow in Porous Media. Proceedings of the XXVI CILAMCE, 2005.

Essenhigh, H., Fundamentals of Coal Combustion, as chapter in "Chemistry of Coal Utilization", volume Secondary supplementary. Willey-Interscience publication, New York, NY, 1981.

Kumar, M.; Garon, A.M. An Experimental Investigation of the Fireflooding

Combustion Zone. Soc. Pet. Eng. Res. Eng., 6 (1), 55-61, 1991.

Mota, J.C.; Marchesin, D.; Dantas, W.B. Combustion Fronts in Porous Media. SIAM Journal on Applied Mathematics, 62 (6), 2175-2198, 2002.

Prats, M. Thermal Recovery. SPE Monograph Series SPE of AIME, 1982.

Press, W. H.; Flannery, B.P; Teukolsky, S.A.; Vetterling, W.T. Numerical Recipes in C. New York: Cambridge University Press, 1989.

Schult, D.A.; Bayliss, A.; Matkowsky, B.J. Traveling Waves in Natural Counterflow Filtration Combustion and Their Stability. SIAM J. Appl. Math, 58 (3), 806-852, 1998.

Souza, A.J.; Marchesin, D.; Akkutlu, I.Y. Wave Sequences for Solid Fuel Adiabatic In-Situ Combustion in Porous Media. Comp. Appl. Math, 25 (1), 27-54, 2006.